

# Tarin-Loaded Nanoliposomes Activate Apoptosis and Autophagy and Inhibit the Migration of Human Mammary Adenocarcinoma Cells

Raiane Vieira Cardoso<sup>1</sup>, Patricia Ribeiro Pereira<sup>1</sup>, Cyntia Silva Freitas<sup>1</sup>, Érika Bertozzi de Aquino Mattos<sup>1</sup>, Anna Victoria De Freitas Silva<sup>2</sup>, Victor do Valle Midlej<sup>2</sup>, Mauricio Afonso Vericimo<sup>3</sup>, Carlos Adam Conte-Júnior<sup>1</sup>, Vania Margaret Flosi Paschoalin<sup>1</sup>

<sup>1</sup>Departamento de Bioquímica, Universidade Federal do Rio de Janeiro, Rio de Janeiro, RJ, Brazil; <sup>2</sup>Instituto Oswaldo Cruz, Rio de Janeiro, RJ, Brazil;

<sup>3</sup>Departamento de Imunobiologia; Universidade Federal Fluminense, Niterói, RJ, Brazil

Correspondence: Vania Margaret Flosi Paschoalin, Av. Athos da Silveira Ramos 149 – sala 545 - Cidade Universitária, Rio de Janeiro, 21941-909, RJ, Brazil, Tel +55(21)3938-7362, Fax +55(21)3938-7266, Email paschv@iq.ufrj.br

**Background:** Tarin, a lectin purified from *Colocasia esculenta*, promotes in vitro and in vivo immunomodulatory effects allied to promising anticancer and antimetastatic effects against human adenocarcinoma mammary cells. This makes this 47 kDa-protein a natural candidate against human breast cancer, a leading cause of death among women. Tarin encapsulated in pegylated nanoliposomes displays increased effectiveness in controlling the proliferation of a mammary adenocarcinoma lineage comprising MDA-MB-231 cells.

**Methods:** The mechanisms enrolled in anticancer and antimetastatic responses were investigated by treating MDA-MB-231 cells with nano-encapsulated tarin at 72 µg/mL for up to 48h through flow cytometry and transmission electron microscopy (TEM). The safety of nano-encapsulated tarin towards healthy tissue was also assessed by the resazurin viability assay, and the effect of nanoencapsulated tarin on cell migration was evaluated by scratch assays.

**Results:** Ultrastructural analyses of MDA-MB-231 cells exposed to nanoencapsulated tarin revealed the accumulation of autophagosomes and damaged organelles, compatible with autophagy-dependent cell death. On the other hand, the flow cytometry investigation detected the increased occurrence of acidic vacuolar organelles, a late autophagosome trait, along with the enhanced presence of apoptotic cells, activated caspase-3/7, and cell cycle arrest at G0/G1. No deleterious effects were observed in healthy fibroblast cells following tarin nanoencapsulated exposition, in contrast to reduced viability in cells exposed to free tarin. The migration of MDA-MB-231 cells was inhibited by nano-encapsulated tarin, with delayed movement by 24 h compared to free tarin.

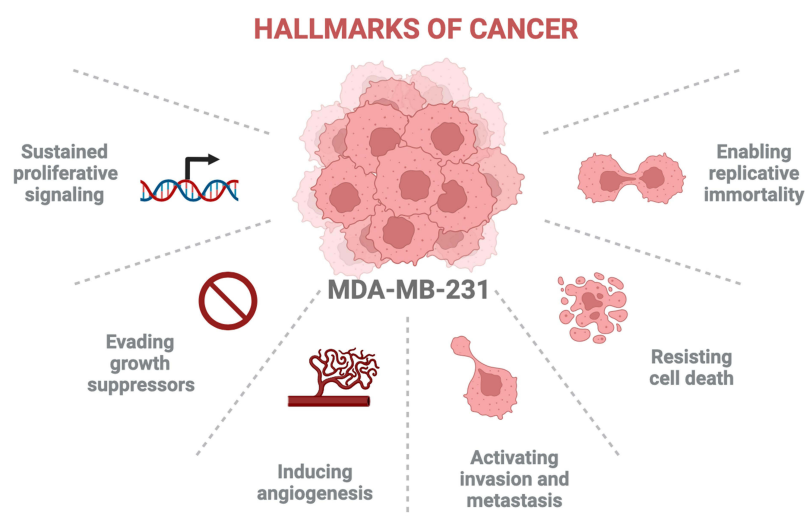
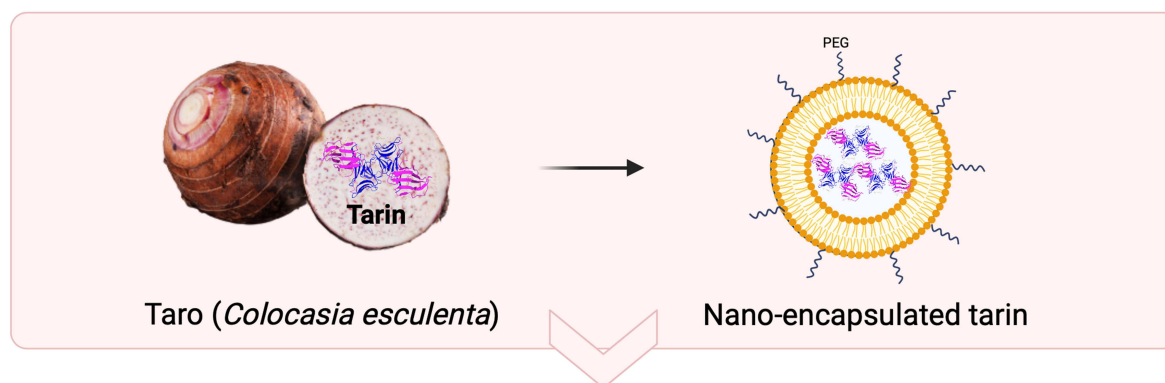
**Conclusion:** The nanoliposome formulation delivers tarin in a delayed and sustained manner, as evidenced by the belated and potent antitumoral and anti-migration effects on adenocarcinoma cells, with no toxicity to healthy cells. Although further investigations are required to fully understand antitumorigenic tarin mechanisms, the activation of both apoptotic and autophagic machineries along with the caspase-3/7 pathway, and cell cycle arrest may comprise a part of these mechanisms.

**Keywords:** tarin-controlled release, MDA-MB-231 cells damage, kinetics of ultrastructural changes, cell cycle arrest, cell migration assay, caspase 3/7 pathway

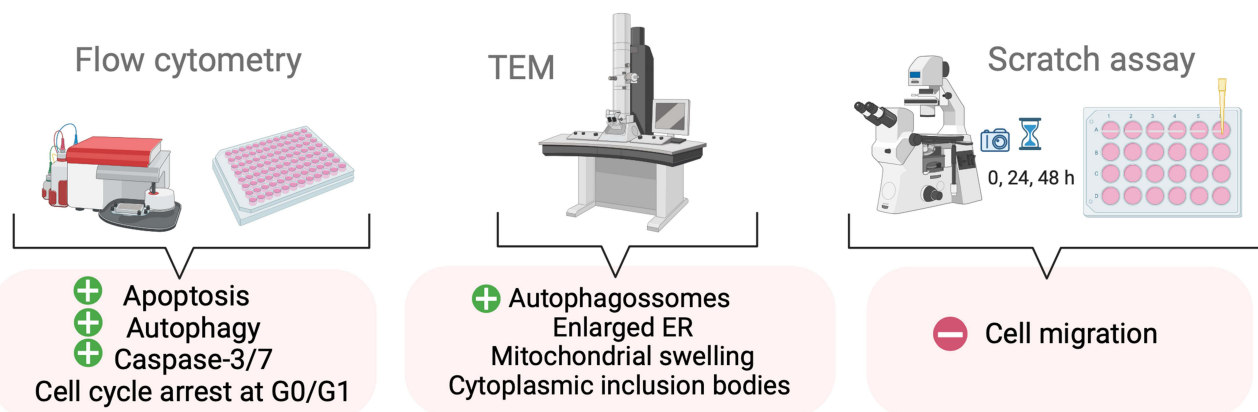
## Introduction

Breast carcinoma comprises approximately 12% of all diagnosed cancers and is the leading cause of death due to cancer among women worldwide according to GLOBOCAN 2020.<sup>1</sup> Oral or intravenous chemotherapy, combined with other therapeutic approaches such as surgery and radiotherapy, are still the most common administration routes of medicines used to treat advanced breast cancer.<sup>2-5</sup> To overcome drug delivery barriers, alternative strategies for drug design drugs and delivery systems have been developed, including liposomes,<sup>6</sup> polymers<sup>7-9</sup> and inorganic nanomaterials.<sup>10</sup> Liposomes have been recognized as a promising and widely employed nanomaterials for the delivery of therapeutic agents, due to

## Graphical Abstract



## Nano-encapsulated tarin mechanisms of controlling cell proliferation



their ability to enhance intracellular drug concentrations in cancer cells while simultaneously reducing toxicity to healthy cells.<sup>11,12</sup> Liposomes can be loaded with hydrophilic and hydrophobic drugs, being composed of biocompatible, biodegradable, and non-immunogenic materials. Moreover, pegylated nano-liposomes can easily pass between

endothelial cells and accumulate in tumor tissues, delivering active antitumorigenic agents. The incorporation of polyethylene glycol (PEG) to nanoliposome formulations provides a substantial advantage by minimizing their recognition by macrophages, preventing their rapid clearance from the bloodstream, giving the formulation the ability to maintain the pharmacological agent for prolonged periods, due to non-significant losses over circulation time.<sup>13,14</sup> In this regard, liposomes, as versatile drug encapsulation delivery platforms, offer a promising solution to minimize toxicity following combined chemotherapy.<sup>15–17</sup> The first liposomal doxorubicin (DOX) formulation, Doxil®, was approved by the Food and Drug Administration (FDA) in 1995 for ovarian cancer treatment, HIV-associated Kaposi's sarcoma, and multiple myeloma, also recently approved for breast cancer therapy in 2016.<sup>18</sup>

From 2015 to 2019, a total of 208 new chemotherapeutic drugs were approved, 58 of them natural compounds, including 15 peptide sequences or peptide-containing molecules.<sup>19,20</sup> These bioactive compounds must be protected from bloodstream proteases, oxidations and other chemical modifications, and their poor solubility in aqueous environments must also be overcome, including intracellular ones.<sup>21</sup> Thus, bioactive proteins and peptides nano-encapsulated into biocompatible carriers are becoming adequate choices to avoid these restrictive physicochemical conditions, used to enhance the half-life and control the release of different compounds.

In this regard, tarin, a four-subunit 47 kDa protein purified from taro (*Colocasia esculenta*) corms and belonging to the *Galanthus nivalis* (GNA)-related lectin family is proven to be an excellent candidate. This lectin has been extensively studied, displaying *in vitro* and *in vivo* immunomodulatory activities, in addition to promising anticancer and antimetastatic effects.<sup>22–29</sup> Indeed, GNA-related lectins are known to promote antitumoral effects in different cell lines via programmed cell death, triggering apoptosis, an intrinsic suicide mechanism regulated by numerous signaling pathways. Autophagy, a cell-breakdown process, may also be triggered, where a multi-step mechanism of lysosomal degradation occurs in damaged proteins and organelles.<sup>30</sup>

In a previous study, nano-encapsulated tarin in pegylated nanoliposomes resulted in a very successful formulation, considering appropriate nanoparticle dimensions for therapeutic applications, as well as nanoparticle stability. The average particle size of tarin loaded nanoliposomes was 154.6 nm, with a polydispersity index (PDI) of 0.168 and an entrapment efficiency of 83%. Furthermore, this formulation achieved controlled tarin release at several pH ranges under distinct physiological environments. It is important to highlight that the nanoencapsulation process fully preserves pharmacological tarin properties, while bioavailability and therapeutic efficacy were improved when tested against different human cancer cell lines, such as glioblastoma (U-87 MG) and mammary adenocarcinoma (MDA-MB-231), with an IC<sub>50</sub> of 39.36 µg/mL and 71.38 µg/mL for each culture at levels comparable to the conventional chemotherapy drugs, cisplatin and temozolomide, and no toxicity observed against mice L929 fibroblasts or bone marrow cells.<sup>23,25,27,31–33</sup> Preliminary data seem to indicate that nano-liposome encapsulation may maintain tarin pharmacological activity during bloodstream transport until reaching the target tissue or organ where tarin can be released, protecting its structure from proteolytic degradation, clearance, and nonspecific interactions, increasing compound half-life and ensuring bioavailability.<sup>34</sup>

In this context, this study aims to investigate the molecular mechanisms underlying the antitumor activity of tarin-loaded nano-liposomes against MDA-MB-231 breast adenocarcinoma cells. Several methodological approaches were employed to this end, including transmission electronic microscopy to monitor ultrastructure morphology tumoral cell changes; flow cytometry to investigate cell death and cell cycle mechanisms and scratch assays to observe cell migration ability when challenged with tarin-loaded nano-liposomes. In summary, this study seeks to demonstrate the promising potential of employing tarin-loaded nanoliposomes as a natural therapeutic adjuvant in cancer treatment.

## Materials and Methods

### Tarin Purification

*C. esculenta* (L.) Schott corms purchased from a local market in Rio de Janeiro, Brazil (22°54'29.9988" S and 43° 11'46.9968" W) were processed to obtain a crude taro extract, as described previously.<sup>35</sup> Taro plant was identified by the botany Marcus A. Nadruz Coelho and a voucher specimen was deposited under the number RFA-39.962 at RFA

Herbarium (<https://specieslink.net/col/RFA>) - Universidade Federal do Rio de Janeiro, Departamento de Botânica, Instituto de Biologia (Rio de Janeiro, RJ, Brazil).<sup>24</sup> Tarin was subsequently purified by affinity chromatography employing a Cibacron Blue 3GA column (Sigma-Aldrich Co, MO, USA) coupled to a Akta purifier 10 Fast Performance Liquid Chromatography (FPLC) system (GE Healthcare, Buckinghamshire, UK).<sup>22</sup> Purified tarin concentrations were estimated using the Total Protein Kit, Micro Lowry, Peterson's modification (Sigma-Aldrich Co, MO, USA) employing bovine serum albumin (BSA) (Sigma-Aldrich Co) as an external standard.

## Preparation of Pegylated Nano-Encapsulated Tarin

Tarin nanoliposome encapsulation was performed through the thin lipid film hydration method as described by early but,<sup>31</sup> with modifications.<sup>36</sup> Nanoliposomes averaging 150 nm and a PDI of  $0.168 \pm 0.03$  were composed of cholesteryl hemisuccinate (CHEMS) (Sigma-Aldrich Co), 1,2-dioleoyl-sn-glycero-3-phosphoethanolamine (DOPE), and [N-(carbonyl-methoxypolyethylene glycol-2000)-1,2-distearoyl-sn-glycero-3-phosphoethanolamine sodium salt] (PEG 2000) (Lipoid, RP, DEU). After encapsulation, the tarin-loaded nano-capsules were separated by ultracentrifugation at  $150,000 \times g$  for 90 min at 4°C (Beckman Coulter, IN, USA) and encapsulation efficiencies were determined as previously described<sup>31</sup> through the quantification of non-encapsulated tarin in the supernatant, employing the Total Protein Kit, Micro Lowry, Peterson's Modification (Sigma-Aldrich Co).

## Human Cell Lines and Culture Conditions

Healthy HFF-1 line human fibroblasts (ATCC SCRC-1041) and MDA-MB-231 line human mammary adenocarcinoma cells (ATCC HTB-26) were obtained from the Rio de Janeiro Cell Bank (BCRJ), RJ, BRA available at <https://bcrl.org.br/>.

The HFF-1 cells were then seeded in 96-well polystyrene microplates at  $5.0 \times 10^5$  cells/mL in 100  $\mu$ L of DMEM High Glucose (Gibco, MA, USA), supplemented with 15% bovine fetal serum (FBS), and incubated at 37°C under a humidified atmosphere containing 5% CO<sub>2</sub> until a semiconfluent monolayer was obtained.

The MDA-MB-231 cells were seeded in 24-well polystyrene plates at  $1.5 \times 10^5$  cells/mL in 1 mL of DMEM-F12 High Glucose (Gibco), supplemented with 10% bovine fetal serum (FBS), and incubated at 37°C under a humidified atmosphere containing 5% CO<sub>2</sub> until a semiconfluent monolayer was obtained.

## Nano-Encapsulated Tarin Cytotoxicity Against HFF-1 Cells

Healthy HFF-1 cell line human fibroblasts were cultivated as mentioned previously for 24 h and 48 h in the presence of increasing free tarin concentrations (3.9  $\mu$ g/mL-500  $\mu$ g/mL), nano-encapsulated tarin (1.67  $\mu$ g/mL-213.25  $\mu$ g/mL) or the corresponding volume of empty liposomes (25%-0.19% v/v). Concerning the positive controls, cells were incubated with sodium azide at 2 mg/mL, while negative controls were incubated in standard media. Cell viability was determined by a colorimetric assay using resazurin at 125  $\mu$ g/mL/well as a growth indicator (Sigma-Aldrich Co.), followed by an additional 4 h of incubation, as described previously.<sup>37</sup> Fluorescence intensities were determined using a Victor™ X microplate reader (PerkinElmer Inc., MA, USA) at 530 and 590 nm excitation and emission wavelengths, respectively.

The viabilities of the MDA-MB-231 cells were previously determined by the redox resazurin method.<sup>31</sup> Subsequent biological assays were performed using a previously determined encapsulated tarin IC<sub>50</sub> value.<sup>31</sup>

## Migration Behavior of MDA-MB-231 Cells Treated with Nano-Encapsulated Tarin

Cell migration was evaluated through the scratch assay.<sup>38</sup> After the MDA-MB-231 culture reached confluence, a linear scratch was generated using a sterile 200  $\mu$ L plastic pipette tip. Cell debris were removed by gentle washing with cold phosphate buffered saline (PBS) at pH 7.4. The cells were then incubated in serum-free DMEM/F12 containing free-tarin (72  $\mu$ g/mL), or nano-encapsulated tarin (72  $\mu$ g/mL), or the equivalent volume of empty liposomes, cyclophosphamide (1 mg/mL) or the standard culture media (control). The scratched area was monitored for 48 h under an inverted trinocular optical microscope (Biofocus, MG, BRA) and photographs were taken. The MDA-MB-231 migration inhibition potential was expressed as the percentage of wounding area corresponding to the ratio between the cell-free area and



the initial area, estimated by the Image J software (public domain software provided by the National Institutes of Health – NIH, MD, USA, available at <https://imagej.nih.gov/ij/download.html>).

## Analysis of Subcellular MDA-MB-231 Morphology Following the Nano-Encapsulated Tarin Challenge

Semiconfluent MDA-MB-23 layers cultivated in 75 cm<sup>3</sup> bottles were incubated for 24 h or 48 h with free tarin (72 µg/mL), or nano-encapsulated tarin (72 µg/mL), or the equivalent volume of empty liposomes or the standard medium (control). Following the incubation, the cell monolayer was washed with warm PBS at pH 7.4 and fixed with 2.5% glutaraldehyde in a 0.1 M sodium-cacodylate buffer at pH 7.4 for 1 h at room temperature. The cells were then post-fixed in a 1% osmium tetroxide (Sigma) and 0.8% potassium ferrocyanide solution and dehydrated using an increasing acetone concentration series (70%, 90%, and 100%) (Merck), embedded in Epon resin, and polymerized at 60°C. Ultrathin sections (60–70 nm thick) were obtained and stained with 5% uranyl acetate (EMS) and lead citrate. The morphological and ultrastructural analyses was performed using an HT7800 RuliTEM microscope (Hitachi, JPN).<sup>39</sup>

## Investigation of Cell Death Mechanisms - Apoptosis and Autophagy - Upon Treatment by Nano-Encapsulated Tarin on MDA-MB-231 Cells

The MDA-MB-231 cells were treated with free or nano-encapsulated tarin, both at 72 µg/mL, or the equivalent volume of empty liposomes, or cyclophosphamide at 1 mg/mL for 24 h and 48 h. After the incubation period, cells were collected by trypsinization and washed with cold PBS at pH 7.4 following centrifugation at 200 × g for 10 min. Cells were then evaluated using the Dead Cell Apoptosis Kit by the Annexin V FITC/propidium iodide (PI) (Thermo Fisher Scientific, MA, USA) assay according to the manufacturer's instructions. Cell pellets were then dispersed in 100 µL of Annexin-binding buffer and stained with 5 µL of FITC Annexin V and 1 µL of a propidium iodide solution at 100µg/mL and incubated at room temperature for 15 min in the dark. Subsequently, 400 µL of 1X Annexin-binding buffer was added and the amounts of necrotic/apoptotic cells were detected employing a BD Accuri C6 plus flow cytometry (BD Bioscience, CA, USA) with the FL-1 (AnnexinV-FITC) and FL-3 (PI) channels.

Cell autophagy was evaluated through the quantification of acidic vacuolar organelles (AVOs) using acridine orange, that glows red in all cell compartments except for acidic ones, such as the mature/late autophagosomes. The MDA-MB-231 cells were exposed to free or nano-encapsulated tarin at 72 µg/mL, with the equivalent volume of empty liposomes or cyclophosphamide at 1 mg/mL for 24 h and 48 h. Briefly, cells were collected by trypsinization, stained with 1 µg/mL acridine orange (Sigma-Aldrich Co.) in a complete culture media (DMEM-F12 High Glucose) for 15 min at room temperature in the dark and analyzed using a BD Accuri C6 plus flow cytometry (BD Bioscience) with the FL-1 vs FL-3 channels to detect red and green fluorescence, expressed as the ratio intensity R/GFIR.<sup>40,41</sup>

## Cell Cycle and Sub-G1 Analysis of MDA-MB-231 Cells Treated by Nano-Encapsulated Tarin

A cell cycle analysis was performed by flow cytometry (BD Bioscience) and DNA staining with PI to measure the number of cells in each MDA-MB-231 cell cycle phase.

Cultivated cells were exposed to free tarin at 72 µg/mL, nano-encapsulated tarin at 72 µg/mL, or the equivalent volume of empty liposomes or cyclophosphamide at 1 mg/mL for 24 h and 48 h. Cells were collected by trypsinization, washed twice in cold PBS at pH 7.4 through centrifugation at 800 × g for 5 min, fixed with 70% ethanol, treated with 50 µL of RNase A at 20 mg/mL (Sigma-Aldrich Co), stained with 200 µL of PI at 50 µg/mL (Sigma-Aldrich Co) and incubated overnight at 4°C.<sup>42</sup> Cell cycle profiles were determined using the BD Accuri C6 plus software. Cells at each cell cycle phase were expressed as percentages.

## Investigation of Caspase-3 and Caspase-7 Activations in MDA-MB-231 Cells Exposed to Nano-Encapsulated Tarin

The MDA-MB-231 cells cultivated according to the aforementioned culture conditions were exposed to free tarin at 72  $\mu\text{g/mL}$ , or nano-encapsulated tarin at 72  $\mu\text{g/mL}$ , or the equivalent volume of empty liposomes or cyclophosphamide at 1 mg/mL for 24 h and 48 h. Following incubation, cells were collected by trypsinization and washed with cold PBS at pH 7.4 by centrifugation at  $200 \times g$  for 10 min. The cell pellets were then dispersed in 250  $\mu\text{L}$  of green caspase-3/7 detection reagent (CellEvent™ Caspase-3/7 (Thermo Fisher Scientific) and incubated at 37°C for 30 min in the dark according to the manufacturer's instructions. Cells were then analyzed by flow cytometry using a BD Accuri C6 plus Flow Cytometer (BD Bioscience) and fluorescence as detected at 502/530 nm absorption/emission wavelengths (FL-1).

### Statistical Analysis

The results were compared by an analysis of variance (ANOVA) followed by multiple comparisons by the Tukey method, or a multiple *t* test followed by the Holm–Sidak method post-test. The GraphPad Prism software version 7 (GraphPad, CA, USA) was used for all statistical analyses, considering  $p < 0.05$  as significant.

## Results and Discussion

### Preservation of Healthy Human Cell Viability Following Nano-Encapsulated Tarin Challenge

Previous data on the antitumoral activity of tarin encapsulated in pegylated nano-liposomes against MDA-MB-231 indicate that the nano-formulation was able to inhibit cell proliferation by 50% ( $\text{IC}_{50}$ ) at 72  $\mu\text{g/mL}$ .<sup>31</sup> Considering this, 72  $\mu\text{g/mL}$  was established to be employed as the reference for the subsequent assays described herein. The nano-encapsulated tarin formulation was shown to be safe for in vivo systems, as healthy human fibroblast cells (HFF-1 lineage) challenged for 24 h and 48 h were not affected, even at concentrations over the  $\text{IC}_{50}$ , ranging from 106.62  $\mu\text{g/mL}$  to 217.5  $\mu\text{g/mL}$ , where healthy cell proliferation was stimulated (Figure 1, upper panels). On the other hand, free tarin from 125 to 500  $\mu\text{g/mL}$  triggered an early cytotoxic fibroblast effect after 24 h (Figure 1, bottom panels), persisting up to 48 h at 500  $\mu\text{g/mL}$ , ie, 7-fold superior to the established  $\text{IC}_{50}$  (Figure 1, bottom panels), indicating irreversible damage to healthy fibroblast cells or the persistence of residual amounts of tarin.

These findings indicate that the encapsulation process is efficient to protect bioactive compounds while minimizing or abolishing the toxic effects promoted by free tarin at the highest investigated concentrations. Nano-encapsulated tarin can, therefore, be safely applied at its effective antitumoral concentration of 72  $\mu\text{g/mL}$  without the threat of adverse effects on surrounding healthy tissues. Moreover, empty liposomes did not interfere with cell viability, evidencing the atotoxicity of the encapsulating material to healthy tissues at the investigated concentrations, as expected for a biocompatible wall nano-capsule material.

### Anti-Migration Effect of Nano-Encapsulated Tarin on Human Breast Adenocarcinoma Cells

Nano-encapsulated tarin inhibited the migration of MDA-MB-231 cells at 72  $\mu\text{g/mL}$  and higher, as indicated by the obtained photomicroscopies and by the estimation of the remaining cell-free area (Figures 2 and 3). Free tarin exhibited a minimal retraction area at 72  $\mu\text{g/mL}$  and no retraction at the highest concentrations. This behavior was accompanied by high toxicity to tumorigenic cells, evidenced by cellular morphology alterations from clustered fibroblastoid (adhered) to rounded forms, indicating neoplastic cell death (Figure S1) early in the first 24 h of exposure, explaining the reported results. Nano-encapsulated tarin also inhibited MDA-MB-231 cell migration at all investigated concentrations, leading to around a 25% retraction area (Figures 2A–C and 3). In contrast to free tarin, which exhibited high toxicity to adenocarcinoma cells, promoting cell death early during the 24 h exposure period and at the lowest concentration, no visual morphological changes indicating cell toxicity were observed following nano-encapsulated tarin exposure on the first 24 h, but instead, late, after 48 h (Figure S1). Empty liposomes did not interfere with migratory cell behavior, but

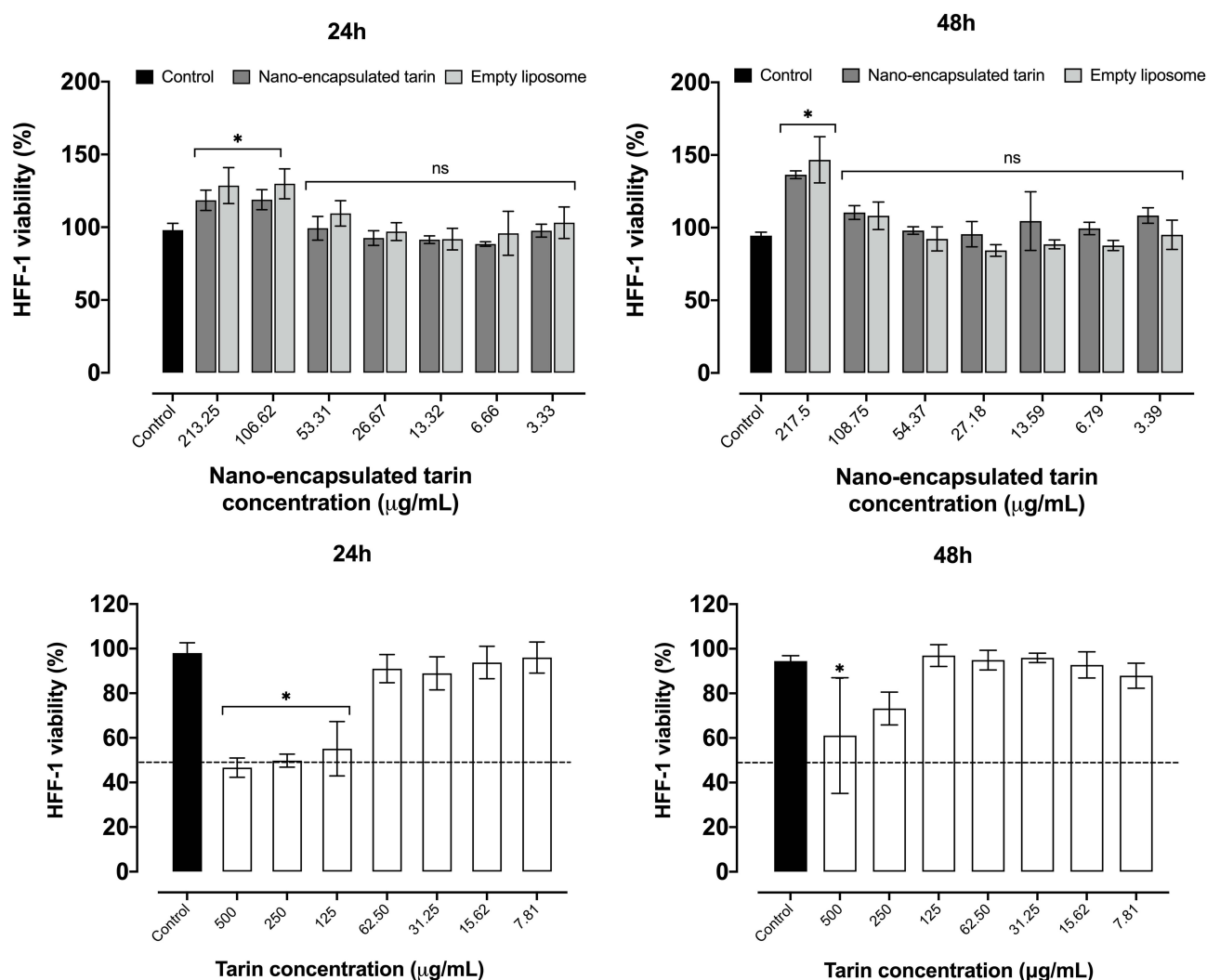


**Figure 1** Viability of healthy human cells (HFF-1) exposed to nanoliposome-encapsulated tarin (upper panels) and free tarin (bottom panels) for 24 h and 48 h. The viability of HFF-1 cells in cultures was determined employing resazurin as an indicator. The x-axis in the upper panel refers to the encapsulated tarin concentration, while empty liposomes refer to the corresponding volume of liposomal solution used to reach that concentration. \* $p < 0.05$  compared to the control. ns – non-significant relative to the control.

indeed presented the same aspect as the control group, where a great number of cells migrated to the scratched area (data not shown), confirming nano-capsule anti-migration non-interference.

The observed anti-migration effects following exposure to free or nano-encapsulated tarin at 72, 144 and 288  $\mu\text{g/mL}$  (Figure 2D) were similar irrespective to the concentration, indicating that both free and nano-encapsulated tarin are effective at the lowest concentration (Figure 2D). Thus, subsequent experiments were performed with nano-encapsulated tarin at 72  $\mu\text{g/mL}$ , the concentration able to trigger anti-migration responses, avoiding undesirable and probable PEG interference and toxicity to healthy cells. The addition of PEG to nanoliposomes aims to increase their stability and circulation in the human body, in addition to improving tumoral tissue targeting, by improving the permeability and retention effect (PRE), capable of enhancing therapeutic effects and reducing loaded drug toxicity.<sup>43,44</sup> However, at high doses, PEG can also cause side effects, as evidence indicates potent immunogenicity of PEG-bearing nanoparticles or biopharmaceuticals.<sup>45</sup> Ishida, Ichihara, Wang, Kiwada,<sup>46</sup> for example, demonstrated that pegylated liposomes trigger anti-PEG IgM production right after the first administration, playing a dominant role in acceleration of the blood clearance phenomenon – ABC.

Cell migration plays a crucial role in cancer metastasis, corresponding to the initial stage, followed by invasion into other tissues, which is the main cause of cancer-related death. To establish metastatic sites, cancer cells must be able to

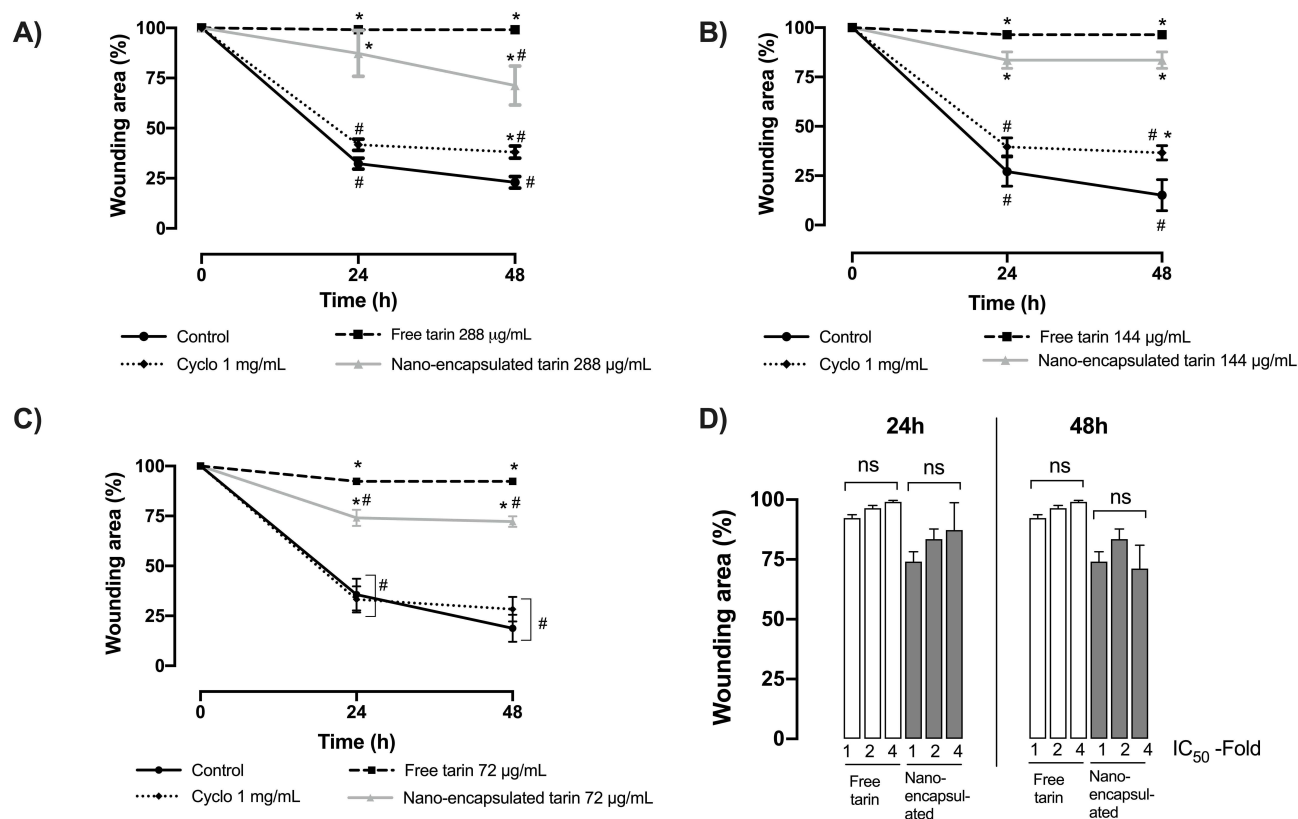


**Figure 2** MDA-MB-231 cell migration kinetics over time estimated by wound areas formed in cell monolayers following exposure to free or nano-encapsulated tarin at 288 µg/mL (A) at 144 µg/mL (B) and at 72 µg/mL (C), after 24 h and 48 h. (D) Intra-group anti-migration effects were compared at 72, 144 and 288 µg/mL, corresponding to 1xIC<sub>50</sub>, 2xIC<sub>50</sub> and 4xIC<sub>50</sub>, respectively. Experiments were performed in triplicate and statistical significances were evaluated by a two-way ANOVA followed by a post-test Tukey's test, considering  $p < 0.05$  as significant. (A–C) \*Represents difference when compared with the control group and #compared with tarin group. (D) ns – non-significant.

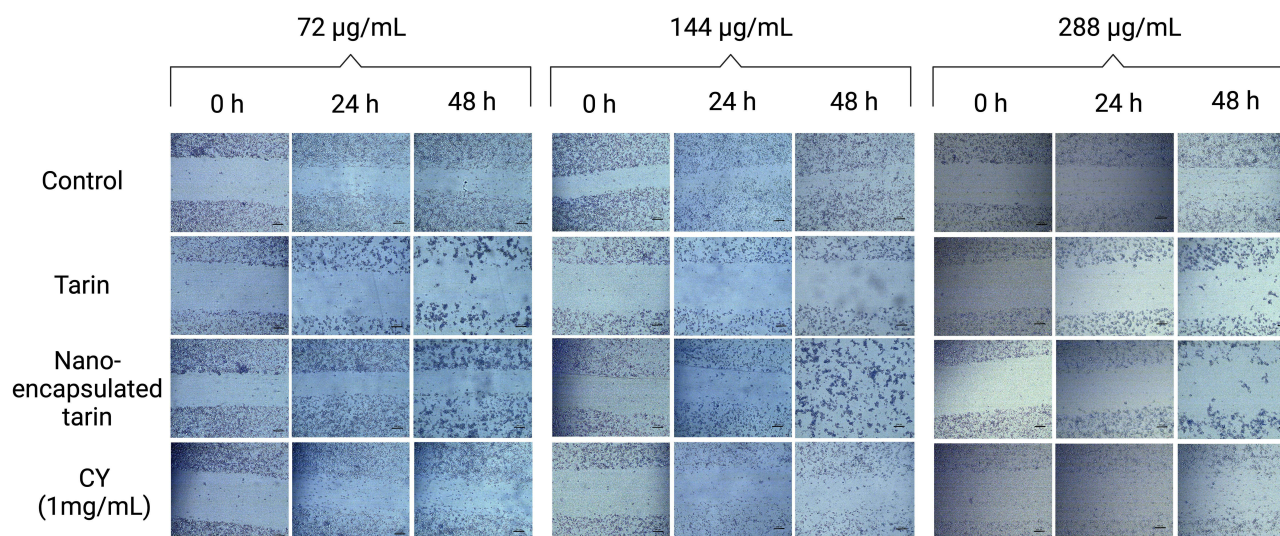


**Figure 3** Migration of MDA-MB-231 adenocarcinoma cells treated with free or nano-encapsulated tarin. Photomicroscopies of the scratched areas were captured at 0 h, 24 h and 48 h after incubation with free tarin or nano-encapsulated tarin at 72, 144 and 288 µg/mL; CY: cyclophosphamide at 1 mg/mL or medium (control). Images were obtained in triplicate under an inverted microscope at a 40x magnification. Scale bars represent 200 µm.

detach from the primary tumor and extend to bloodstream to colonize other organs or tissues.<sup>47–49</sup> Kundu, Campbell, Hampton, Lin, Ma, Ambulos, Zhao, Goloubeva, Holt, Fulton<sup>27</sup> have demonstrated that tarin can inhibit or minimize the colonization of lungs and heart in the murine breast cancer line 66.1, respectively, conferring a potent anti-metastatic



effect to tarin. The results reported herein indicate that tarin nano-encapsulation can preserve tarin anti-migration effect, while also delaying cytotoxic effects as a consequence of the controlled and sustained release of the tarin loaded into nano-liposomes (Figures 2 and 3), suggesting that this nano-formulation may retain the original anti-metastatic potential of free-tarin.

## Ultrastructural Changes Associated to Autophagy in Human MDA-MB-231 Cells Caused by Nano-Encapsulated Tarin

The antitumoral effect of plant lectins, especially GNA- family members, including tarin, is widely reported and considered a remarkable functional characteristic of these proteins.<sup>30,50–52</sup> Antitumoral tarin effects have been evidenced against various neoplastic cell lines, including human breast cancer, hepatoma and glioblastoma, in which it prevented secondary colonization sites, as mentioned previously.<sup>28,33,53</sup> However, its antitumorigenic mechanisms are still unrevealed, especially regarding the novel tarin nano-formulation investigated herein. Ultrastructural changes in MDA-MB-231 breast cancer cells induced by free or nano-encapsulated tarin over 48 h were analyzed through transmission electron microscopy (TEM) following apoptosis/autophagy investigation assays.

MDA-MB-231 cells challenged by nano-encapsulated tarin at 72 µg/mL for 24 h (Figure 4, left panel) revealed the presence of autophagosomes (Figure 4c–f, left panel, black arrows) frequently found as endoplasmic reticulum profiles wrapped in cytoplasm sub-structures like mitochondria. After 48 h (Figure 4, right panel), extensive damage was evidenced by endoplasmic reticulum enlargement (Figure 4c', right panel, black arrow), mitochondrial swelling (Figure 4d', right panel, arrowhead) and the presence of cytoplasmic inclusion bodies around the nucleus (Figure 4d'–f', right panel, asterisks). Autophagosome accumulation indicates the activation of a cell death process through autophagy.<sup>54</sup> The repetitive autophagosome pattern in cells treated with nano-encapsulated tarin (Figure 4c–f,

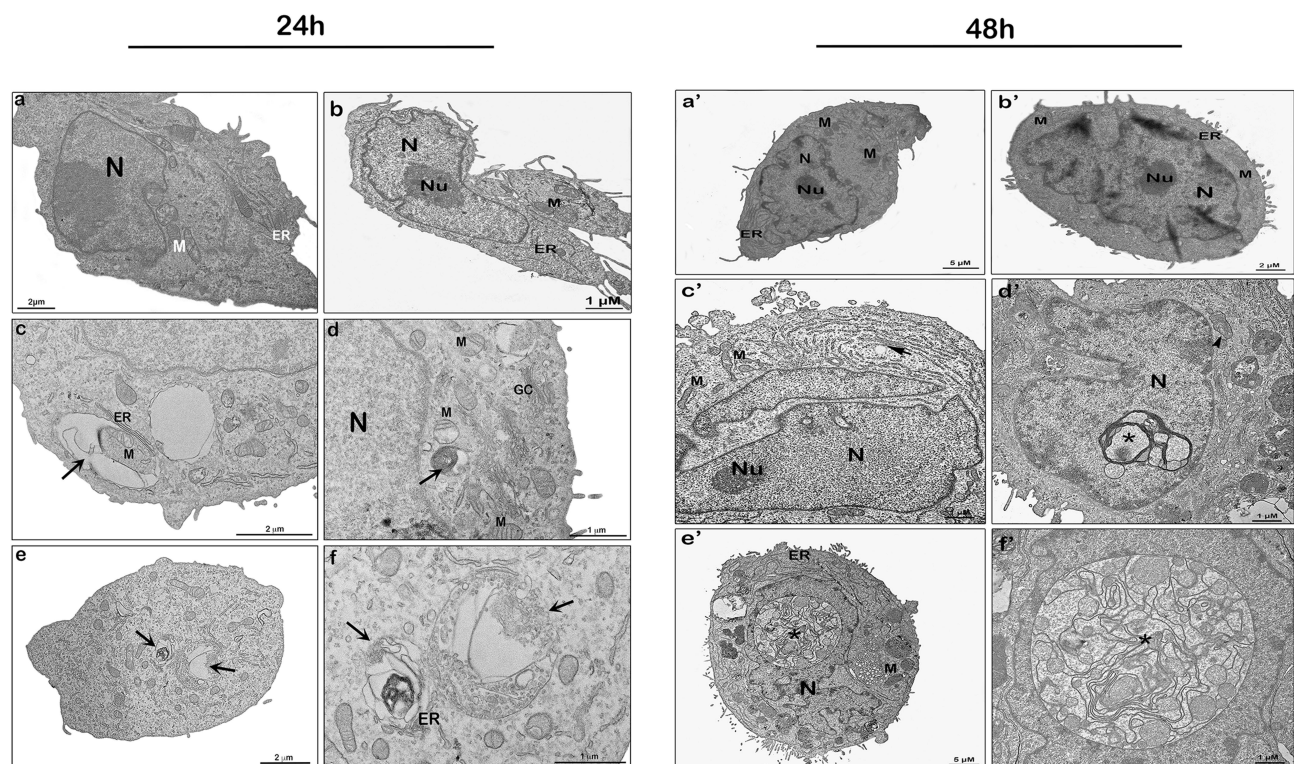


**Figure 4** Ultrastructure of MDA-MB-231 cells treated by nano-encapsulated tarin and analyzed through transmission electron microscopy after 24 h (left panel) and 48 h (right panel) of exposition. Control (a, a'), empty liposome (b, b'), and nano-encapsulated tarin at 72 µg/mL (c-f, c'-f'). Autophagosomes are indicated by the black arrows in the left panel; enlarged endoplasmic reticula, by the black arrow in the right panel; mitochondrial swelling, by the black arrowhead; and cytoplasmic inclusion bodies near the nucleus, by asterisks.

**Abbreviations:** ER, endoplasmic reticulum; N, nucleus; Nu, nucleolus; CG, Golgi complex; M, mitochondria.



left panel) is compatible with the inhibition observed in cell migration assays (Figures 2 and 3), where well-preserved cells can still apparently be found after 24 h.

Cells exposed to empty liposomes (Figure 4b, b') and control cells (Figures 4a, a' and 5a, b) shared similar morphological characteristics, exhibiting well-preserved structures, such as mitochondria (M), endoplasmic reticulum (ER) profiles, nucleus (N) and nucleolus (Nu), Golgi complex (GC), as well as a homogeneous cytoplasm. On the other hand, cells treated with 72 µg/mL of free tarin for 24 h (Figure 5c–f) exhibited cytoplasmic content extravasation (\*) and endoplasmic reticulum enlargement and distension (white arrowhead) (Figure 5e), indicating cell death, corroborating the cell death evidence observed in the migration assays (Figures 2 and 3).

Considering that tarin encapsulated in nano-liposomes is released in a controlled manner, the results reported herein may indicate that autophagy represents an initial cell death step, whereas the morphological changes promoted by free tarin could represent the final death process stage. These findings are in accordance with anticancer responses reported for other GNA-related lectins, which exert cancer cell death through the apoptosis or autophagy activation, as well as autophagy-dependent apoptosis, through the activation of mitochondrial ROS–p38–p53 and caspase-dependent pathways or blocking of the Ras–Raf and PI3K–Akt pathways.<sup>30,55,56</sup> In this regard, additional investigations should be conducted to determine if apoptosis, in addition to autophagy, can also be activated by nano-encapsulated tarin and if free tarin triggers similar mechanisms.

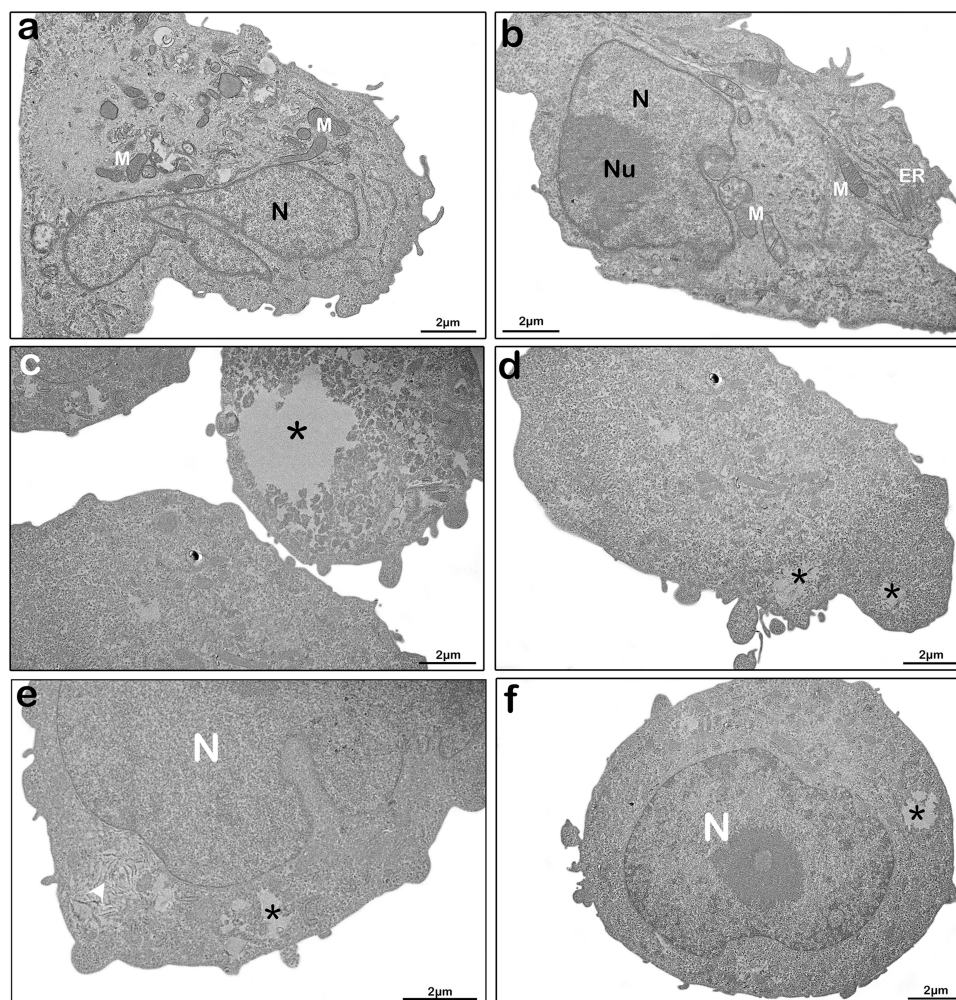


**Figure 5** Ultrastructure changes in MDA-MB-231 cells treated with free-tarin. Ultrastructural images by transmission electron microscopy of untreated (a-b) and treated cells with free tarin at 72 µg/mL for 24 h (c-f). \*cytoplasm extravasation; white arrow, enlargement and distension of endoplasmic reticula.

**Abbreviations:** ER, endoplasmic reticulum; N, nucleus; Nu, nucleolus; M, mitochondria.

Cells treated with free or nano-encapsulated tarin were stained with acridine orange followed by a flow cytometry analysis for the detection of acid vacuolar organelles (Figure 6). In accordance with the TEM assessments, MDA-MB-231 cells exhibited a significant increase in acidic vacuolar organelles, indicating the presence of late autophagosomes after 24 h of treatment with 72  $\mu\text{g/mL}$  of nano-encapsulated tarin, increasing up to 48 h (Figure 6). Interestingly, free tarin was also able to stimulate the formation of autophagosomes, indicating that the taro lectin in either free or nano-encapsulated form may cause cell death by autophagy, similarly to other GNA-related lectins.<sup>30,55,56</sup>

## Apoptosis in MDA-MB-231 Cells Challenged with Nano-Encapsulated Tarin

The MDA-MB-231 cells previously exposed to nano-encapsulated tarin at 72  $\mu\text{g/mL}$  for 24 h or 48 h were stained with Annexin V-FITC and PI for the detection of apoptotic cells (Figures 7 and S2).

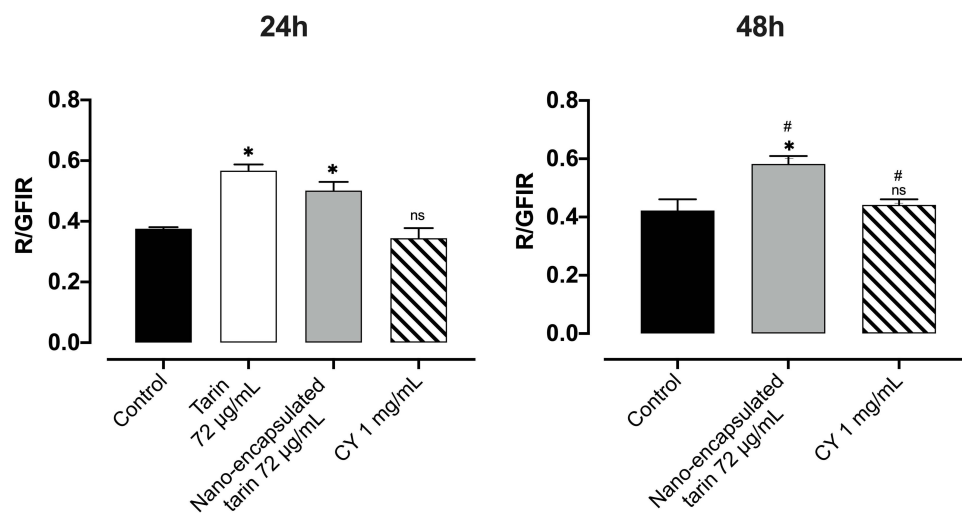


**Figure 6** Cell death in MDA-MB-231 cultures treated by encapsulated tarin at 72  $\mu\text{g/mL}$  for 24 h (left panel) and 48 h (right panel) stained by acridine Orange and analyzed by flow cytometry to detect acidic vesicular organelles, representing late/intermediate autophagosomes. Results were expressed as a red-to-green fluorescence intensity ratio (R/GFIR). Experiments were performed in triplicate, where \* represents a significant difference compared to the control group and, # compared to the same group at 24 h with  $p < 0.05$ . CY – cyclophosphamide at 1 mg/mL.

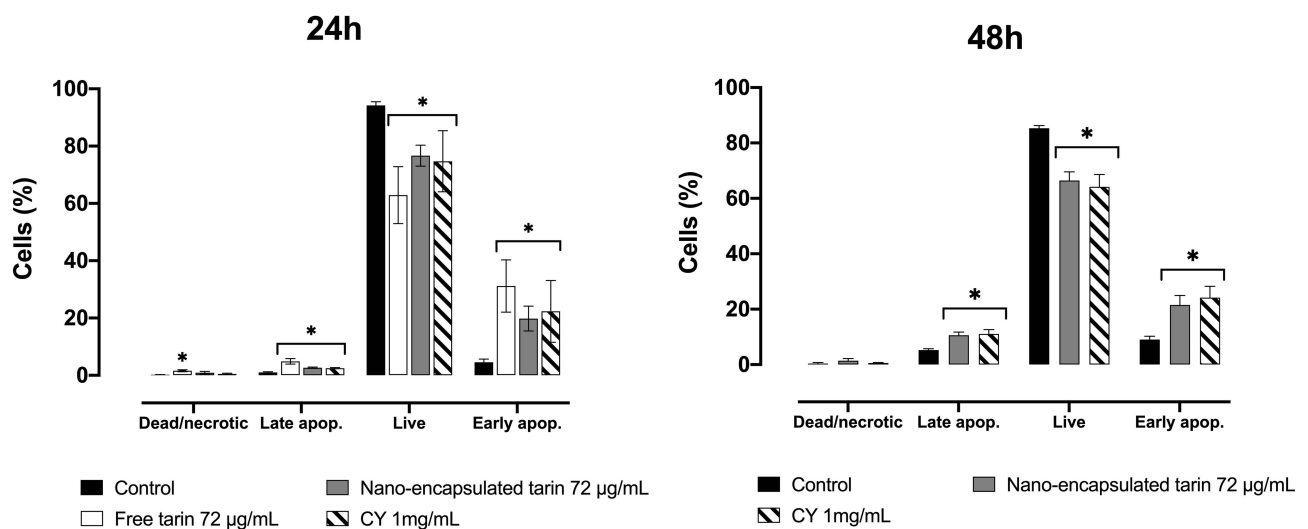


**Figure 7** Apoptotic cells in MDA-MB-231 cultures exposed to 72  $\mu\text{g/mL}$  of nano-encapsulated tarin for 24 h (left panel) or 48 h (right panel). The percentages of dead or necrotic, early apoptotic, live, and late apoptotic cells were assessed by staining cells with annexin V-FITC and PI followed by flow cytometry analyses. Fluorescence was detected in the FL-1-H (FITC) and FL-3-H (PI) channels. Experiments were performed in triplicate, where \* denotes a significant difference compared to the control. CY – cyclophosphamide.

A significant increase in the percentage of cells in early and late apoptosis stages was observed after a 24 h treatment with free tarin or nano-encapsulated tarin at 72  $\mu\text{g/mL}$  (Figure 7, left panel). However, unlike what was observed for nano-encapsulated tarin, free tarin promoted apoptosis in a higher percentage of cells and increased the percentage of necrotic cells. Thus, it seems that free-tarin causes apoptosis and accelerates death in cells already in the apoptotic phase, promoting necrosis. After 48 h, the percentage of cells in an early and late apoptosis stage significantly increased from untreated cells (control) (Figure 7, right panel), while no significant increase in dead/necrotic cells after exposure to nano-encapsulated tarin for 48 h was observed.

Apoptosis, also termed type I programmed cell death, is essential for the homeostasis of cell populations through cell turnover and the elimination of unwanted cells, as a defense mechanism against toxins and diseases. On the other hand, autophagy, a natural cytoprotective process, maintains homeostasis by promoting cell survival by the elimination of damaged organelles or macromolecules and by recycling of cell components, providing health/alive cells with nutrients and energy. In healthy tissues, apoptosis and autophagy occurs in a coordinated manner to guarantee homeostatic equilibrium between cell death and survival. However, excess autophagy stimuli can lead to cell death, also known as type II programmed cell death.<sup>57,58</sup>

Cancer cells display dysregulated machinery, with the over-expression of anti-apoptotic proteins that enable them to over-proliferate while escaping apoptosis cell death with the aid of autophagy. Accumulated evidence indicates that autophagy and apoptosis can also occur as connected mechanisms, sharing many signaling mediators and interplaying in three distinct manners: *i*) simultaneously, in a synergic or in a collaborative manner inducing cell death or *ii*) autophagy can promote apoptosis culminating in cell death, or *iii*) autophagy antagonizes apoptosis or vice-versa, promoting cell survival. Various therapeutical agents target the induction of the first two mechanisms to control cell proliferation, used for cancer treatment.<sup>59,60</sup>

Lectins obtained from *Polygonatum odoratum* and *Polygonatum cyrtoneura*, belonging to GNA-related family lectins, share the same  $\beta$ -prism II structure with tarin, as well as the conserved motif on the carbohydrate binding site. Up to now, these were the only GNA-related lectins reported to induce both autophagy and apoptosis in human MCF-7 breast cancer cells, melanoma A375 cells and lung adenocarcinoma A549 cells.<sup>61–65</sup> Our results, however, indicate that tarin, a GNA-related lectin from taro, is also able to trigger antitumoral activity through the activation of autophagy and apoptosis in MDA-MB-231 cells, although it is not clear if these mechanisms are linked, and if so, if the interaction occurs via collaborative/synergistic or promoting effects.

## Studying the Apoptosis Mechanisms Through the Activation of Caspase-3/7

The activation of caspase 3 and caspase 7 was investigated in MDA-MB-231 cells treated with nano-encapsulated tarin for 24 h and 48 h (Figures 8 and S3). An increase in the percentage of cells containing activated caspase-3/7 was observed after a 24h-challenge with free or nano-encapsulated tarin, but significantly lower in the encapsulated form (Figure 8, left panel). Interestingly, the nano-encapsulated tarin caused an additional increment in caspase activation after 48 h, reaching the effect observed for free tarin at 24 h. These results corroborate and confirms that tarin can also cause cell death by apoptosis, which is dependent on the activation of the caspase 3/7 pathway. Furthermore, the controlled release of tarin from nano-liposomes is clearly evidenced by the significant delayed effect on the activation of caspase 3 and caspase 7 when compared to free tarin.

The activations of caspase-3 and caspase-7 are irreversibly related to apoptosis cell death and are a downstream mediator resulted from the signaling molecules caspase 9 or caspase 8. Activated caspase 3 splices PARP, inactivating it and subsequently triggering apoptosis.<sup>59</sup> Caspase 9 participates in the intrinsic apoptotic pathway stimulated by mitochondrial damage with subsequent cytochrome c release and caspase 9 activation. Caspase-8 is a part of the extrinsic apoptotic pathway that depends on the stimulation of death receptors, such as Fas (CD95), tumor necrosis factor receptor 1 (TNFR1) or TNF-related apoptosis-inducing ligand receptor (TRAILR).<sup>58</sup> Moreover, caspase 3 activation may also be associated to the autophagy process, as ATG4D, an ATG4 protease isoform that belongs to the autophagy-related proteins (ATGs) family, is also a substrate for caspase 3, whose action gives rise to a cleaved isoform, leading to autophagy.<sup>66</sup> Herein, it is not clear if apoptosis and autophagy are both linked to caspase 3 activation, although it is undoubtedly being activated. Further studies are required to understand the involved tarin upstream signaling pathways and to clarify if both

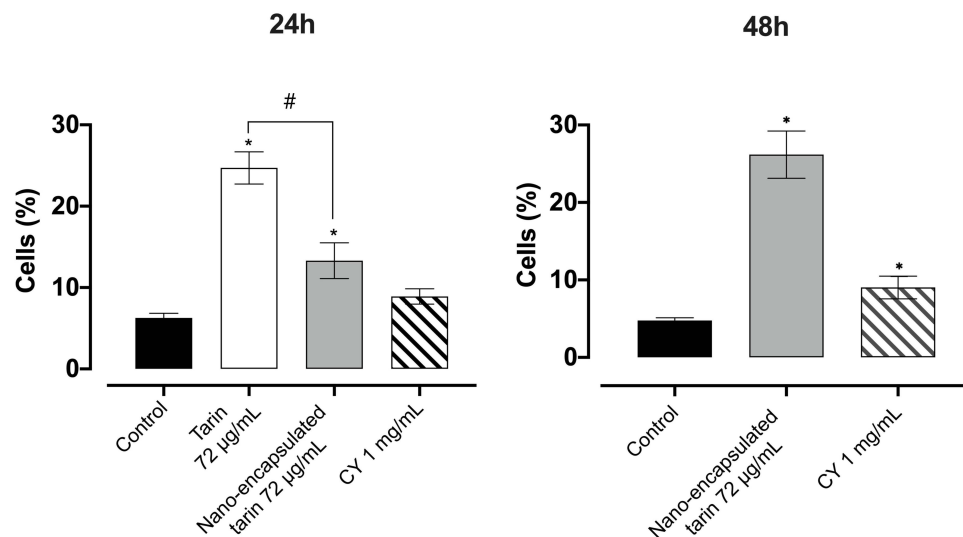


**Figure 8** Activation of caspase 3 and caspase 7 in MDA-MB-231 cells treated with nano-encapsulated tarin at 72 µg/mL for 24 h (left panel) and 48 h (right panel). The percentage of cells containing activated caspases 3/7 was inferred using a fluorogenic tetrapeptide substrate (DEVD) conjugated to a green dye. The fluorescence signal was captured through a flow cytometer in the FL-I channel. Experiments were performed in triplicate. \*represents significant difference compared to the control group or # compared to tarin, with  $p < 0.05$ . CY- cyclophosphamide at 1 mg/mL.

death cell mechanisms occur simultaneously or if one is promoting the other. Proteomic analyses are already in progress and will provide a full comprehension on the expression of intracellular proteins to correlate with the present findings, especially if autophagy is linked to caspase 3 activation, and to address other open questions. Furthermore, cellular uptake studies are also important to determine the interaction kinetics and the optimal cargo of liposomes, as well as to prospect modifications in the nanoliposome design to enhance cell interaction and uptake.

## Effect of Nano-Encapsulated Tarin on the MDA-MB-231 Cell Cycle

Apoptotic cells and alterations in MDA-MB-231 cell cycle phases after the nano-encapsulated tarin challenge for 24 h and 48 h were evaluated by flow cytometry in PI-stained cells (Figures 9 and S4). An increase in sub-G1 cells treated with 72 µg/mL free tarin was observed after 24 h, while no effect was observed in cells treated with nano-encapsulated tarin (Figure 9, left panel). On the other hand, no increase in sub-G1 cells was detected after 48 h of exposure to free or nano-encapsulated tarin (Figure 9, right panel). Encapsulated and free tarin did not alter cell cycle phases following 24 h exposure, except for tarin, which exhibited a slight decrease in G0/G1 phase cells (Figure 9, left panel). However, nano-encapsulated tarin triggered significant alterations in all cell cycle phases, with the accumulation of cells in G0/G1

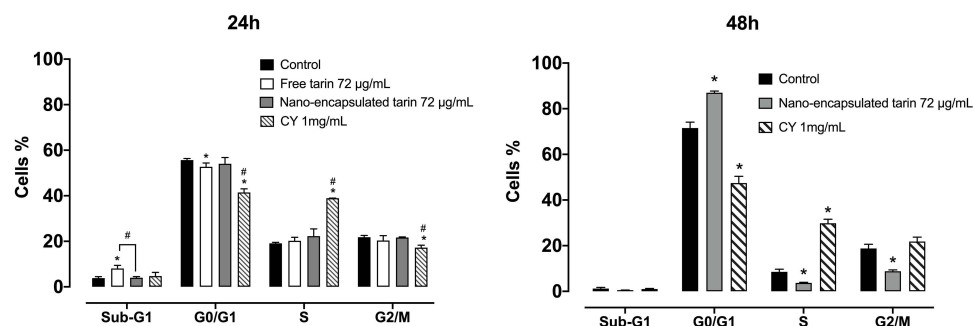


**Figure 9** Cell cycle phases and sub-G1 cells of MDA-MB-231 cultures treated by encapsulated tarin at 72 µg/mL for 24h and 48h. Cells were stained with PI and fluorescence was detected by flow cytometry in the FL-2 channel. All experiments were performed in triplicate. \*indicates significant difference compared to the control, and #, compared to tarin, with  $p < 0.05$ . CY- cyclophosphamide at 1 mg/mL.



and consequent decrease in the S and G2/M phases (Figure 9, right panel), indicating that the cell cycle arrest at G0/G1 impairs the proliferation of neoplastic cells.

## Conclusion

The nano-encapsulated tarin formulation, at 72 µg/mL, its effective antitumorigenic dose, was proven safe for healthy human tissues (HFF-1). Nanoencapsulated tarin did not adversely affect the viability of healthy cells and provided a protective effect against cytotoxicity induced by free tarin. Furthermore, tarin exhibited inhibitory breast cancer cell migration properties, which was delayed in the nano-encapsulated formulation, indicating a controlled and sustained tarin release from nanoliposomes. The mechanisms underlying tarin-induced MDA-MB-231 cell death involves both apoptotic and autophagic pathways, including the activation of caspase 3/7 pathway, cell cycle arrest and the formation of acidic vacuolar organelles, characteristic of autophagosomes. Although nano-encapsulated tarin exhibits promising potential as a natural adjuvant agent in chemotherapy for breast cancer treatment, further investigations are required to gain a comprehensive understanding of the molecular mechanisms underlying cancer cell death mediated by the nano-encapsulated tarin formulation, as well as the signaling pathways involved in this process.

## Author Contributions

All authors made significant contributions to this study reported, whether study conception, design, execution, data acquisition, analysis and interpretation, or in all these areas; took part in drafting, revising or critically reviewing the article; gave final approval of the version to be published; have agreed on the journal to which the article has been submitted; and agree to be accountable for all aspects of the work.

## Funding

This research was funded by Fundação Carlos Chagas Filho de Amparo à Pesquisa do Estado do Rio de Janeiro (FAPERJ), grant number E-26/202.254/2018, E-26/210.865/2019, E-26/201.016/2021, E-26/210.093/2023, E-26/010.000.984/2019; E-26/204.372/2021, E-26/204.373/2021; E-26/200.756/2023; Conselho Nacional de Desenvolvimento Científico e Tecnológico (CNPq), grant number 140020/2021-7.

## Disclosure

The authors report no conflicts of interest in this work.

## References

1. Antoniou AI, Giofrè S, Seneci P, Passarella D, Pellegrino S. Stimulus-responsive liposomes for biomedical applications. *Drug Discov Today*. 2021;26(8):1794–1824. doi:10.1016/j.drudis.2021.05.010
2. Al-Mahmood S, Sapiezynski J, Garbuzenko OB, Minko T. Metastatic and triple-negative breast cancer: challenges and treatment options. *Drug Deliv Transl Res*. 2018;8:1483–1507. doi:10.1007/s13346-018-0551-3
3. Waks AG, Winer EP. Breast cancer treatment: a review. *JAMA*. 2019;321(3):288–300. doi:10.1001/jama.2018.19323
4. Sharifi M, Jafari S, Hasan A, et al. Antimetastatic activity of lactoferrin-coated mesoporous maghemite nanoparticles in breast cancer enabled by combination therapy. *ACS Biomater Sci Eng*. 2020;6(6):3574–3584. doi:10.1021/acsbiomaterials.0c00086
5. ElOuassif B, Idri A, Hosni M, Abran A. Classification techniques in breast cancer diagnosis: a systematic literature review. *Comput Methods Biomech Biomed Eng Imaging Vis*. 2021;9(1):50–77.
6. Vahed SZ, Salehi R, Davaran S, Sharifi S. Liposome-based drug co-delivery systems in cancer cells. *Mater Sci Eng C*. 2017;71:1327–1341. doi:10.1016/j.msec.2016.11.073
7. Zuris JA, Thompson DB, Shu Y, et al. Cationic lipid-mediated delivery of proteins enables efficient protein-based genome editing in vitro and in vivo. *Nat Biotechnol*. 2015;33(1):73–80. doi:10.1038/nbt.3081
8. Wang M, Zuris JA, Meng F, et al. Efficient delivery of genome-editing proteins using bioreducible lipid nanoparticles. *Proc Natl Acad Sci*. 2016;113(11):2868–2873. doi:10.1073/pnas.1520244113
9. Chen W, Deng W, Goldys EM. Light-triggerable liposomes for enhanced endolysosomal escape and gene silencing in PC12 cells. *Mol Ther Nucleic Acids*. 2017;7:366–377. doi:10.1016/j.omtn.2017.04.015
10. Xiao H, Li C, Dai Y, Cheng Z, Hou Z, Lin J. Inorganic nanocarriers for platinum drug delivery. *Mater Today*. 2015;18(10):554–564. doi:10.1016/j.mattod.2015.05.017
11. Pattni BS, Chupin VV, Torchilin VP. New developments in liposomal drug delivery. *Chem Rev*. 2015;115(19):10938–10966. doi:10.1021/acs.chemrev.5b00046
12. Zylberberg C, Gaskill K, Pasley S, Matosevic S. Engineering liposomal nanoparticles for targeted gene therapy. *Gene Ther*. 2017;24(8):441–452. doi:10.1038/gt.2017.41



13. Weis SM, Cheresh DA. Tumor angiogenesis: molecular pathways and therapeutic targets. *Nat Med*. 2011;17(11):1359–1370. doi:10.1038/nm.2537
14. Woodle M, Collins L, Sponsler E, Kossovsky N, Papahadjopoulos D, Martin F. Sterically stabilized liposomes. Reduction in electrophoretic mobility but not electrostatic surface potential. *Biophys J*. 1992;61(4):902–910. doi:10.1016/S0006-3495(92)81897-0
15. Zhao M, Ding X-F, Shen J-Y, Zhang X-P, Ding X-W, Xu B. Use of liposomal doxorubicin for adjuvant chemotherapy of breast cancer in clinical practice. *J Zhejiang Univ Sci B*. 2017;18(1):15. doi:10.1631/jzus.B1600303
16. Din F, Aman W, Ullah I, et al. Effective use of nanocarriers as drug delivery systems for the treatment of selected tumors. *Int J Nanomedicine*. 2017;12:7291–7309. doi:10.2147/IJN.S146315
17. Dong M, Luo L, Ying X, et al. Comparable efficacy and less toxicity of pegylated liposomal doxorubicin versus epirubicin for neoadjuvant chemotherapy of breast cancer: a case-control study. *Onco Targets Ther*. 2018;11:4247–4252. doi:10.2147/OTT.S162003
18. Gabizon AA, Patil Y, La-Beck NM. New insights and evolving role of pegylated liposomal doxorubicin in cancer therapy. *Drug Resist Updat*. 2016;29:90–106. doi:10.1016/j.drug.2016.10.003
19. Haddadzadegan S, Dorkoosh F, Bernkop-Schnürch A. Oral delivery of therapeutic peptides and proteins: technology landscape of lipid-based nanocarriers. *Adv Drug Deliv Rev*. 2022;182:114097. doi:10.1016/j.addr.2021.114097
20. Jain D, Mahammad SS, Singh PP, Kodipyaka R. A review on parenteral delivery of peptides and proteins. *Drug Dev Ind Pharm*. 2019;45(9):1403–1420. doi:10.1080/03639045.2019.1628770
21. Bruno BJ, Miller GD, Lim CS. Basics and recent advances in peptide and protein drug delivery. *Ther Deliv*. 2013;4(11):1443–1467. doi:10.4155/tde.13.104
22. Pereira PR, Del Aguila EM, Verícimo MA, Zingali RB, Paschoalin VMF, Silva JT. Purification and characterization of the lectin from taro (*Colocasia esculenta*) and its effect on mouse splenocyte proliferation in vitro and in vivo. *Protein J*. 2014;33:92–99. doi:10.1007/s10930-013-9541-y
23. Pereira PR, Winter HC, Verícimo MA, et al. Structural analysis and binding properties of isoforms of tarin, the GNA-related lectin from *Colocasia esculenta*. *Biochim Biophys Acta*. 2015;1854(1):20–30. doi:10.1016/j.bbapap.2014.10.013
24. Pereira PR, Silva JT, Verícimo MA, Paschoalin VM, Teixeira GA. Crude extract from taro (*Colocasia esculenta*) as a natural source of bioactive proteins able to stimulate haematopoietic cells in two murine models. *J Funct Foods*. 2015;18:333–343. doi:10.1016/j.jff.2015.07.014
25. Pereira PR, Meagher JL, Winter HC, et al. High-resolution crystal structures of *Colocasia esculenta* tarin lectin. *Glycobiology*. 2017;27(1):50–56. doi:10.1093/glycob/cww083
26. Sang Chan Y, Ho Wong J, Bun Ng T. A cytokine-inducing hemagglutinin from small taros. *Protein Pept Lett*. 2010;17(7):823–830. doi:10.2174/092986610791306742
27. Kundu N, Campbell P, Hampton B, et al. Antimetastatic activity isolated from *Colocasia esculenta* (taro). *Anticancer Drugs*. 2012;23(2):200–211. doi:10.1097/CAD.0b013e32834b85e8
28. Pereira PR, Corrêa ACNTE, Verícimo MA, Paschoalin VMF. Tarin, a potential immunomodulator and COX-inhibitor lectin found in taro (*Colocasia esculenta*). *Compr Rev Food Sci Food Saf*. 2018;17(4):878–891. doi:10.1111/1541-4337.12358
29. Mérida LA, Mattos ÉB, Corrêa AC, et al. Tarin stimulates granulocyte growth in bone marrow cell cultures and minimizes immunosuppression by cyclo-phosphamide in mice. *PLoS One*. 2018;13(11):e0206240. doi:10.1371/journal.pone.0206240
30. Wu L, Bao J-K. Anti-tumor and anti-viral activities of *Galanthus nivalis* agglutinin (GNA)-related lectins. *Glycoconj J*. 2013;30:269–279. doi:10.1007/s10719-012-9440-z
31. Corrêa AC, Verícimo MA, Dashevskiy A, Pereira PR, Paschoalin VM. Liposomal taro lectin nanocapsules control human glioblastoma and mammary adenocarcinoma cell proliferation. *Molecules*. 2019;24(3):471. doi:10.3390/molecules24030471
32. Corrêa AC, Pereira PR, Paschoalin VM. Preparation and characterization of nanoliposomes for the entrapment of bioactive hydrophilic globular proteins. *JoVE*. 2019;150:e59900.
33. Kundu N, Ma X, Hoag S, et al. An extract of taro (*Colocasia esculenta*) mediates potent inhibitory actions on metastatic and cancer stem cells by tumor cell-autonomous and immune-dependent mechanisms. *Breast Cancer*. 2021;15:11782234211034937. doi:10.1177/11782234211034937
34. Yasin U, Bilal M, Bashir H, Amirzada MI, Sumrin A, Asad MHHB. Preparation and nanoencapsulation of lectin from *Lepidium sativum* on chitosan-tripolyphosphate nanoparticle and their cytotoxicity against hepatocellular carcinoma cells (HepG2). *Biomed Res Int*. 2020;2020:1–11. doi:10.1155/2020/7251346
35. Roy A, Banerjee S, Majumder P, Das S. Efficiency of mannose-binding plant lectins in controlling a homopteran insect, the red cotton bug. *J Agric Food Chem*. 2002;50(23):6775–6779. doi:10.1021/jf025660x
36. Dos Santos Ferreira D, Faria SD, de Araújo Lopes SC, et al. Development of a bone-targeted pH-sensitive liposomal formulation containing doxorubicin: physicochemical characterization, cytotoxicity, and biodistribution evaluation in a mouse model of bone metastasis. *Int J Nanomedicine*. 2016;11:3737. doi:10.2147/IJN.S109966
37. McMillian M, Li L, Parker J, et al. An improved resazurin-based cytotoxicity assay for hepatic cells. *Cell Biol Toxicol*. 2002;18:157–173. doi:10.1023/A:1015559603643
38. Grada A, Otero-Vinas M, Prieto-Castrillo F, Obagi Z, Falanga V. Research techniques made simple: analysis of collective cell migration using the wound healing assay. *J Invest Dermatol*. 2017;137(2):e11–e16. doi:10.1016/j.jid.2016.11.020
39. Diniz Filho JFS, de Barros A, Pijera MSO, et al. Ultrastructural analysis of cancer cells treated with the radiopharmaceutical radium dichloride ([223Ra]RaCl<sub>2</sub>): understanding the effect on cell structure. *Cells*. 2023;12(3):451. doi:10.3390/cells12030451
40. Filippi-Chiela EC, Villodre ES, Zamin LL, Lenz G. Autophagy interplay with apoptosis and cell cycle regulation in the growth inhibiting effect of resveratrol in glioma cells. *PLoS One*. 2011;6(6):e20849. doi:10.1371/journal.pone.0020849
41. Jiang H, White EJ, Conrad C, Gomez-Manzano C, Fueyo J. Autophagy pathways in glioblastoma. *Methods Enzymol*. 2009;453:273–286.
42. Hu Z-Y, Sun J, Zhu X-F, Yang D, Zeng Y-X. ApoG2 induces cell cycle arrest of nasopharyngeal carcinoma cells by suppressing the c-Myc signaling pathway. *J Transl Med*. 2009;7:1–11. doi:10.1186/1479-5876-7-74
43. Maruyama K. Intracellular targeting delivery of liposomal drugs to solid tumors based on EPR effects. *Adv Drug Deliv Rev*. 2011;63(3):161–169. doi:10.1016/j.addr.2010.09.003
44. Milla P, Dosio F, Cattel L. PEGylation of proteins and liposomes: a powerful and flexible strategy to improve the drug delivery. *Curr Drug Metab*. 2012;13(1):105–119. doi:10.2174/138920012798356934
45. Shiraishi K, Yokoyama M. Toxicity and immunogenicity concerns related to PEGylated-micelle carrier systems: a review. *Sci Technol Adv Mater*. 2019;20(1):324–336. doi:10.1080/14686996.2019.1590126

46. Ishida T, Ichihara M, Wang X, Kiwada H. Spleen plays an important role in the induction of accelerated blood clearance of PEGylated liposomes. *J Control Release*. 2006;115(3):243–250. doi:10.1016/j.jconrel.2006.08.001
47. Wu J-S, Jiang J, Chen B-J, Wang K, Tang Y-L, Liang X-H. Plasticity of cancer cell invasion: patterns and mechanisms. *Transl Oncol*. 2021;14(1):100899. doi:10.1016/j.tranon.2020.100899
48. Gupta GP, Massagué J. Cancer metastasis: building a framework. *Cell*. 2006;127(4):679–695. doi:10.1016/j.cell.2006.11.001
49. Fares J, Fares MY, Khachfe HH, Salhab HA, Fares Y. Molecular principles of metastasis: a hallmark of cancer revisited. *Signal Transduct Target Ther*. 2020;5(1):28. doi:10.1038/s41392-020-0134-x
50. Liu Z, Luo Y, Zhou -T-T, Zhang W-Z. Could plant lectins become promising anti-tumour drugs for causing autophagic cell death? *Cell Prolif*. 2013;46(5):509–515. doi:10.1111/cpr.12054
51. Mazalovska M, Kouokam JC. Plant-derived lectins as potential cancer therapeutics and diagnostic tools. *Biomed Res Int*. 2020;2020:1631394. doi:10.1155/2020/1631394
52. Li C-Y, Meng L, Liu B, Bao J-K. Galanthus nivalis agglutinin (GNA)-related lectins: traditional proteins, burgeoning drugs? *Curr Chem Biol*. 2009;3(3):323–333. doi:10.2174/187231309789054913
53. Ribeiro Pereira P, Bertozzi de Aquino Mattos É, Nitzsche Teixeira Fernandes Correa AC, Afonso Vericimo M, Margaret Flosi Paschoalin V. Anticancer and Immunomodulatory Benefits of Taro (*Colocasia esculenta*) Corms, an underexploited tuber crop. *Int J Mol Sci*. 2020;22(1):265. doi:10.3390/ijms22010265
54. Mizushima N, Yoshimori T, Levine B. Methods in mammalian autophagy research. *Cell*. 2010;140(3):313–326. doi:10.1016/j.cell.2010.01.028
55. Yau T, Dan X, Ng CCW, Ng TB. Lectins with potential for anti-cancer therapy. *Molecules*. 2015;20(3):3791–3810. doi:10.3390/molecules20033791
56. Bhutia SK, Panda PK, Sinha N, et al. Plant lectins in cancer therapeutics: targeting apoptosis and autophagy-dependent cell death. *Pharmacol Res*. 2019;144:8–18. doi:10.1016/j.phrs.2019.04.001
57. Xi H, Wang S, Wang B, et al. The role of interaction between autophagy and apoptosis in tumorigenesis (Review). *Oncol Rep*. 2022;48(6):208. doi:10.3892/or.2022.8423
58. Das S, Shukla N, Singh SS, Kushwaha S, Shrivastava R. Mechanism of interaction between autophagy and apoptosis in cancer. *Apoptosis*. 2021;26(9):512–533. doi:10.1007/s10495-021-01687-9
59. Xie Q, Liu Y, Li X. The interaction mechanism between autophagy and apoptosis in colon cancer. *Transl Oncol*. 2020;13(12):100871. doi:10.1016/j.tranon.2020.100871
60. Su M, Mei Y, Sinha S. Role of the crosstalk between autophagy and apoptosis in cancer. *J Oncol*. 2013;2013:102735. doi:10.1155/2013/102735
61. Wang S-Y, Yu Q-J, Bao J-K, Liu B. Polygonatum cyrtonema lectin, a potential antineoplastic drug targeting programmed cell death pathways. *Biochem Biophys Res Commun*. 2011;406(4):497–500. doi:10.1016/j.bbrc.2011.02.049
62. Ouyang L, Chen Y, Wang X-Y, et al. Polygonatum odoratum lectin induces apoptosis and autophagy via targeting EGFR-mediated Ras-Raf-MEK-ERK pathway in human MCF-7 breast cancer cells. *Phytomedicine*. 2014;21(12):1658–1665. doi:10.1016/j.phymed.2014.08.002
63. Liu B, Cheng Y, Zhang B, Bian H-J, Bao J-K. Polygonatum cyrtonema lectin induces apoptosis and autophagy in human melanoma A375 cells through a mitochondria-mediated ROS-p38-p53 pathway. *Cancer Lett*. 2009;275(1):54–60. doi:10.1016/j.canlet.2008.09.042
64. Liu T, Wu L, Wang D, et al. Role of reactive oxygen species-mediated MAPK and NF-κB activation in polygonatum cyrtonema lectin-induced apoptosis and autophagy in human lung adenocarcinoma A549 cells. *J Biochem*. 2016;160(6):315–324. doi:10.1093/jb/mvw040
65. Wu L, Liu T, Xiao Y, et al. Polygonatum odoratum lectin induces apoptosis and autophagy by regulation of microRNA-1290 and microRNA-15a-3p in human lung adenocarcinoma A549 cells. *Int J Biol Macromol*. 2016;85:217–226. doi:10.1016/j.ijbiomac.2015.11.014
66. Tsapras P, Nezis IP. Caspase involvement in autophagy. *Cell Death Differ*. 2017;24(8):1369–1379. doi:10.1038/cdd.2017.43